ROBUST FAULT TOLERANT CONTROL WITH SENSOR FAULTS FOR A FOUR-ROTOR HELICOPTER

Hicham Khebbache[1], Belkacem Sait[2] and Fouad Yacef [3]
[1,2] Automatic Laboratory of Setif (LAS), Electrical Engineering Department,
Setif University, ALGERIA
[3] Automatic Laboratory of Jijel (LAJ), Automatic Control Department,
Jijel University, ALGERIA

ABSTRACT

This paper considers the control problem for an under actuated quadrotor UAV system in presence of sensor faults. Dynamic modelling of quadrotor while taking into account various physical phenomena, which can influence the dynamics of a flying structure is presented. Subsequently, a new control strategy based on robust integral backstepping approach using sliding mode and taking into account the sensor faults is developed. Lyapunov based stability analysis shows that the proposed control strategy design keep the stability of the closed loop dynamics of the quadrotor UAV even after the presence of sensor failures. Numerical simulation results are provided to show the good tracking performance of proposed control laws.

KEYWORDS: *Backstepping control, Dynamic modelling, Fault tolerant control (FTC), Nonlinear systems, Robust control, Quadrotor, Unmanned aerial vehicles (UAV).*

I. INTRODUCTION

Unmanned aerial vehicles (UAV) have shown a growing interest thanks to recent technological projections, especially those related to instrumentation. They made possible the design of powerful systems (mini drones) endowed with real capacities of autonomous navigation at reasonable cost.
Despite the real progress made, researchers must still deal with serious difficulties, related to the control of such systems, particularly, in the presence of atmospheric turbulences. In addition, the navigation problem is complex and requires the perception of an often constrained and evolutionary environment, especially in the case of low-altitude flights.
In contrast to terrestrial mobile robots, for which it is often possible to limit the model to kinematics, the control of aerial robots (quadrotor) requires dynamics in order to account for gravity effects and aerodynamic forces [10].
In [6-13], authors propose a control law based on the choice of a stabilizing Lyapunov function ensuring the desired tracking trajectories along (X,Z) axis and roll angle only. The authors in [2], do not take into account frictions due to the aerodynamic torques nor drag forces. They propose control-laws based on backstepping, and on sliding mode control in order to stabilize the complete system (i.e. translation and orientation). In [16-17], authors take into account the gyroscopic effects and show that the classical model-independent PD controller can stabilize asymptotically the attitude of the quadrotor aircraft. Moreover, they used a new Lyapunov function, which leads to an exponentially stabilizing controller based upon the PD^2 and the compensation of coriolis and gyroscopic torques. While in [9] the authors develop a PID controller in order to stabilize altitude. The authors in [4] propose a control algorithm based upon sliding mode using backstepping approach allowed the tracking of the various desired trajectories expressed in term of the center of mass coordinates along (X,Y,Z) axis and yaw angle. In [8], authors used a controller design based on backstepping approach. Moreover, they introduced two neural nets to estimate the aerodynamic components, one for aerodynamic forces and one for aerodynamic moments. While in [7] the authors propose a hybrid backstepping control technique and the Frenet-Serret Theory (Backstepping+FST) for attitude stabilization, that includes estimation of the desired angular acceleration (within the control law) as a

function of the aircraft velocity. However, all control strategies previously proposed do not take into account the failures affecting the sensors of quadrotor, wich makes them very limited and induces undesired behavior of quadrotor, or even to instability of the latter after occurence of sensor faults.
In this paper, we consider the stabilization problem of the quadrotor aircraft in presence of sensor failures. The dynamical model describing the quadrotor aircraft motions and taking into a account for various parameters which affect the dynamics of a flying structure such as frictions due to the aerodynamic torques, drag forces along (X,Y,Z) axis and gyroscopic effects is presented. Subsequently, a new control strategy based on robust integral backstepping approach using sliding mode taking into account the sensor faults is proposed and compared with a classical backstepping approach. This control strategy includes two compensation techniques, the first technique using an integral action, the second, is to use an another term containing "sign" function to compensate the effect of sensor faults. Finally all synthesized control laws are highlighted by simulations, a comparison with control strategies developed in this paper is also performed, these simulations show the inefficiency of classical backstepping approach after occurrence of sensor faults. Otherwise, fairly satisfactory results despite the presence of this sensor faults are given by the new control strategy.

II. MODELLING

2.1. Quadrotor dynamic modelling

The quadrotor have four propellers in cross configuration. The two pairs of propellers {1,3} and {2,4} as described in Fig. 1, turn in opposite directions. By varying the rotor speed, one can change the lift force and create motion. Thus, increasing or decreasing the four propeller's speeds together generates vertical motion. Changing the 2 and 4 propeller's speed conversely produces roll rotation coupled with lateral motion. Pitch rotation and the corresponding lateral motion; result from 1 and 3 propeller's speed conversely modified. Yaw rotation is more subtle, as it results from the difference in the counter-torque between each pair of propellers.
Let E (0,x,y,z) denote an inertial frame, and B (0',X,Y,Z) denote a frame rigidly attached to the quadrotor as shown in Fig. 1.

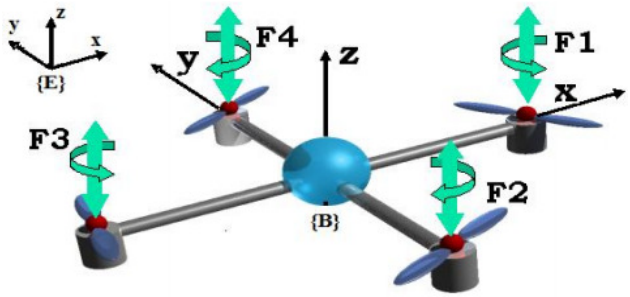

Figure. 1. Quadrotor configuration

Using Euler angles parameterization [12], the airframe orientation in space is given by a rotation matrix R from R^B to R^E.

$$R = \begin{bmatrix} c\psi c\theta & s\phi s\theta c\psi - s\psi c\phi & c\phi s\theta c\psi + s\psi s\phi \\ s\psi c\theta & s\phi s\theta s\psi + c\psi c\theta & c\phi s\theta s\psi - s\phi c\psi \\ -s\theta & s\phi c\theta & c\phi c\theta \end{bmatrix} \quad (1)$$

where C and S indicate the trigonometrically functions **cos** and **sin** respectively.

The dynamic equations based on the formalism of Newton-Euler are given by:

$$\begin{cases} \dot{\zeta} = \nu \\ m\ddot{\zeta} = F_f + F_t + F_g \\ \dot{R} = RS(\Omega) \\ I\dot{\Omega} = -\Omega \wedge I\Omega - M_{gh} - M_a + M_f \end{cases} \quad (2)$$

$S(\Omega)$ is a skew-symmetric matrix; for a given vector $\Omega=[\Omega_1 \quad \Omega_2 \quad \Omega_3]^T$ it is defined as follows:

$$S(\Omega)=\begin{bmatrix} 0 & -\Omega_3 & \Omega_2 \\ \Omega_3 & 0 & -\Omega_1 \\ -\Omega_2 & \Omega_1 & 0 \end{bmatrix} \tag{3}$$

The approximate model of the quadrotor can be rewritten as:

$$\begin{cases} \dot{\zeta} = v \\ m\ddot{\zeta} = R \times \begin{bmatrix} 0 & 0 & \sum_{i=1}^{4} \left(b\omega_i^2\right) \end{bmatrix}^T + K_{ft} v - mge_z \\ \dot{R} = RS(\Omega) \\ I\dot{\Omega} = -\Omega \wedge I\Omega - \sum_{1}^{4} \Omega \wedge J_r \begin{bmatrix} 0 & 0 & (-1)^{i+1}\omega_i \end{bmatrix}^T - K_{fa}\Omega^2 + M_f \end{cases} \tag{4}$$

where:

m	total mass of the structure
$\zeta=[x, y, z]^T$	position vector
v	linear velocity
ϕ	roll angle
θ	pitch angle
Ψ	law angle
Ω	angular velocity
ω_i	angular rotor speed
F_f	resultant of the forces generated by the four rotors
F_t	resultant of the drag forces along (x,y,z) axis
F_g	gravity force
M_{gh}	resultant of torques due to the gyroscopic effects
M_a	resultant of aerodynamics frictions torques
M_f	moment developed by the quadrotor according to the body fixed frame
$K_{ft(x,y,z)}$	translation drag coefficients
$K_{fa(x,y,z)}$	frictions aerodynamics coefficients
$I_{(x,y,z)}$	body inertia
J_r	rotor inertia
b	lift coefficient
d	drag coefficient
l	distance from the rotors to the center of mass of the quadrotor aircraft

The moment developed by the quadrotor according to the body fixed frame along an axis is the difference between the torque generated by each propeller on the other axis.

$$M_f = \begin{bmatrix} lb(\omega_4^2 - \omega_2^2) \\ lb(\omega_3^2 - \omega_1^2) \\ d\left(\omega_1^2 - \omega_2^2 + \omega_3^2 - \omega_4^2\right) \end{bmatrix} \tag{5}$$

The complete dynamic model which governs the quadrotor is as follows [3-4]:

$$\begin{cases} \ddot{\phi} = \dfrac{(I_y - I_z)}{I_x}\dot{\theta}\dot{\psi} - \dfrac{J_r}{I_x}\bar{\Omega}_r\dot{\theta} - \dfrac{K_{fax}}{I_x}\dot{\phi}^2 + \dfrac{l}{I_x}u_2 \\ \ddot{\theta} = \dfrac{(I_z - I_x)}{I_y}\dot{\phi}\dot{\psi} + \dfrac{J_r}{I_y}\bar{\Omega}_r\dot{\phi} - \dfrac{K_{fay}}{I_y}\dot{\theta}^2 + \dfrac{l}{I_y}u_3 \\ \ddot{\psi} = \dfrac{(I_x - I_y)}{I_z}\dot{\theta}\dot{\phi} - \dfrac{K_{faz}}{I_z}\dot{\psi}^2 + \dfrac{1}{I_z}u_4 \\ \ddot{x} = -\dfrac{K_{ftx}}{m}\dot{x} + \dfrac{1}{m}u_x u_1 \\ \ddot{y} = -\dfrac{K_{fty}}{m}\dot{y} + \dfrac{1}{m}u_y u_1 \\ \ddot{z} = -\dfrac{K_{ftz}}{m}\dot{z} - g + \dfrac{\cos(\phi)\cos(\theta)}{m}u_1 \end{cases} \quad (6)$$

with

$$\begin{cases} u_x = (\cos\phi\cos\psi\sin\theta + \sin\phi\sin\psi) \\ u_y = (\cos\phi\sin\theta\sin\psi - \sin\phi\cos\psi) \end{cases} \quad (7)$$

The system's inputs are posed u_1, u_2, u_3, u_4 and $\bar{\Omega}_r$ a disturbance, obtaining:

$$\begin{cases} u_1 = b\left(\omega_1^2 + \omega_2^2 + \omega_3^2 + \omega_4^2\right) \\ u_2 = lb(\omega_4^2 - \omega_2^2) \\ u_3 = lb(\omega_3^2 - \omega_1^2) \\ u_4 = d\left(\omega_1^2 - \omega_2^2 + \omega_3^2 - \omega_4^2\right) \\ \bar{\Omega}_r = \omega_1 - \omega_2 + \omega_3 - \omega_4 \end{cases} \quad (8)$$

From (7) it easy to show that :

$$\begin{cases} \phi_d = \arcsin\left(u_x \sin(\psi_d) - u_y \cos(\psi_d)\right) \\ \theta_d = \arcsin\left(\dfrac{\left(u_x \cos(\psi_d) + u_y \sin(\psi_d)\right)}{\cos(\phi_d)}\right) \end{cases} \quad (9)$$

2.2. Rotor dynamic model

The rotors are driven by DC motors with the well known equations:

$$\begin{cases} v = Ri + L\dfrac{di}{dt} + k_e\omega \\ k_m i = J_r\dfrac{d\omega}{dt} + C_s + k_r\omega^2 \end{cases} \quad (10)$$

As we a small motor with a very low inductance, then we can obtain the voltage to be applied to each motor as follows [9]:

$$v_i = \frac{1}{\eta}\left(\dot{\omega}_i + \mu_0\omega_i^2 + \mu_1\omega_i + \mu_2\right), \mathrm{i} \in [1,...,4] \quad (11)$$

with: $\mu_0 = \dfrac{k_r}{J_r}$, $\mu_1 = \dfrac{k_e k_m}{J_r R}$, $\mu_2 = \dfrac{C_s}{J_r}$ and $\eta = \dfrac{k_m}{J_r R}$

where, v_i : is the motor input, ω : is the angular speed, k_r : is the load torque constant, k_e, k_m : are respectively the electrical and mechanical torque constants, and C_s : is the solid friction.

III. CONTROL STRATEGIES OF QUADROTOR

3.1. Backstepping control of quadrotor

The model (6) presented in the first part of this paper can be written in the state-space form:

$$\dot{X} = f(X, U) \tag{12}$$

with $X \in \Re^n$ is the state vector of the system, such as:

$$X = [x_1, ..., x_{12}]^T = \left[\phi, \dot{\phi}, \theta, \dot{\theta}, \psi, \dot{\psi}, x, \dot{x}, y, \dot{y}, z, \dot{z}\right]^T \tag{13}$$

From (6) and (13) we obtain:

$$f(X, U) = \begin{pmatrix} x_2 \\ a_1 x_4 x_6 + a_2 x_2^2 + a_3 \bar{\Omega}_r x_4 + b_1 u_2 \\ x_4 \\ a_4 x_2 x_6 + a_5 x_4^2 + a_6 \bar{\Omega}_r x_2 + b_2 u_3 \\ x_6 \\ a_7 x_2 x_4 + a_8 x_6^2 + b_3 u_4 \\ x_8 \\ a_9 x_8 + \frac{1}{m} u_x u_1 \\ x_{10} \\ a_{10} x_{10} + \frac{1}{m} u_y u_1 \\ x_{12} \\ a_{11} x_{12} + \frac{\cos(\phi)\cos(\theta)}{m} u_1 - g \end{pmatrix} \tag{14}$$

with

$$\begin{cases} a_1 = \left(\frac{I_y - I_z}{I_x}\right), a_2 = -\frac{K_{fax}}{I_x}, a_3 = -\frac{J_r}{I_x} \\ a_4 = \left(\frac{I_z - I_x}{I_y}\right), a_5 = -\frac{K_{fay}}{I_y}, a_6 = \frac{J_r}{I_y} \\ a_7 = \left(\frac{I_x - I_y}{I_z}\right), a_8 = -\frac{K_{faz}}{I_z}, a_9 - \frac{K_{ftx}}{m},\ a_{10} = -\frac{K_{fty}}{m}, a_{11} = -\frac{K_{ftz}}{m} \\ b_1 = \frac{l}{I_x}, b_2 = \frac{l}{I_y}, b_3 = \frac{1}{I_z} \end{cases} \tag{15}$$

The adopted control strategy is summarized in the control of two subsystems; the first relates to the orientation control, taking into account the position control along (*X*,*Y*) axis, while the second is that of the attitude control as shown it below the synoptic:

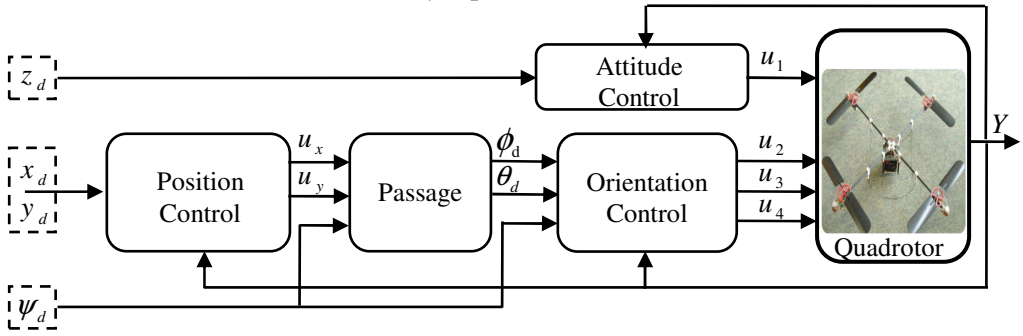

Figure. 2. Synoptic scheme of the proposed control strategy

Using the backstepping approach for the control-laws synthesis, we simplify all the stages of calculation concerning the tracking errors and Lyapunov functions in the following way (Refer to [3] for more details):

$$e_i = \begin{cases} x_{id} - x_i & \text{i} \in [1,3,5,7,9,11] \\ \dot{x}_{(i-1)d} + k_{(i-1)} e_{(i-1)} - x_i & \text{i} \in [2,4,6,8,10,12] \end{cases} \tag{16}$$

and

$$V_i = \begin{cases} \frac{1}{2} e_i^2 & \text{i} \in [1,3,5,7,9,11] \\ V_{i-1} + \frac{1}{2} e_i^2 & \text{i} \in [2,4,6,8,10,12] \end{cases} \tag{17}$$

such as: $k_i > 0,\ \text{i} \in [1,...,12]$

The synthesized stabilizing control laws are as follows:

$$\begin{cases} u_2 = \frac{1}{b_1}\left(\ddot{\phi}_d + k_1(-k_1 e_1 + e_2) + e_1 + k_2 e_2 - a_1 x_4 x_6 - a_2 x_2^2 - a_3 \bar{\Omega}_r x_4\right) \\ u_3 = \frac{1}{b_2}\left(\ddot{\theta}_d + k_3(-k_3 e_3 + e_4) + e_3 + k_4 e_4 - a_4 x_2 x_6 - a_5 x_4^2 - a_6 \bar{\Omega}_r x_2\right) \\ u_4 = \frac{1}{b_3}\left(\ddot{\psi}_d + k_5(-k_5 e_5 + e_6) + e_5 + k_6 e_6 - a_7 x_2 x_4 - a_8 x_6^2\right) \\ u_x = \frac{m}{u_1}\left(\ddot{x}_d + k_7(-k_7 e_7 + e_8) + e_7 + k_8 e_8 - a_9 x_8\right) \quad / u_1 \neq 0 \\ u_y = \frac{m}{u_1}\left(\ddot{y}_d + k_9(-k_9 e_9 + e_{10}) + e_9 + k_{10} e_{10} - a_{10} x_{10}\right) \quad / u_1 \neq 0 \\ u_1 = \frac{m}{\cos(x_1)\cos(x_3)}\left(\ddot{z}_d + k_{11}(-k_{11} e_{11} + e_{12}) + e_{11} + k_{12} e_{12} - a_{11} x_{12} + g\right) \end{cases} \tag{18}$$

3.2. Robust fault tolerant control with sensor faults of quadrotor

The choice of this method is not fortuitous considering the major advantages it presents:

- It ensures Lyapunov stability.
- It ensures the handling of all system nonlinearities.
- It ensures the robustness and all properties of the desired dynamics in presence of sensor faults.

The complete model resulting by adding the sensor faults in the model (6) can be written in the state-space form:

$$\begin{cases} \dot{X} = f(X, U) \\ Y = CX + E_s F_s \end{cases} \tag{19}$$

with $Y \in \Re^p$ is the measured output vector, $F_s \in \Re^q$ is the sensor faults vector, $C \in \Re^{p \times n}$ and $E_s \in \Re^{p \times q}$ are respectively, the observation matrix and the sensor faults distributions matrix.

Remark 1: In our contribution, only the velocity sensor faults are considered, they are assumed to be bounded and slowly varying in time (i.e. $|f_{s_i}| \leq f_{s0}$ and $\dot{f}_{si} \approx 0$).

Consequently :

$$y = [x_1 \quad x_2 + f_{s1} \quad x_3 \quad x_4 + f_{s2} \quad x_5 \quad x_6 + f_{s3} \quad x_7 \quad x_8 + f_{s4} \quad x_9 \quad x_{10} + f_{s5} \quad x_{11} \quad x_{12} + f_{s6}]^T \tag{20}$$

Basing on backstepping approach, a recursive algorithm is used to synthesize the control laws forcing the system to follow the desired trajectory in presence of velocity sensor faults. For the first step we consider the tracking-error:

$$e_1 = x_{1d} - x_1 \tag{21}$$

And we use the Lyapunov theorem by considering the Lyapunov function e_1 positive definite and it's time derivative negative semi-definite:

$$V_1 = \frac{1}{2}e_1^2 + \frac{1}{2}\tilde{d}_1^2 \Big/ \tilde{d}_1 = \frac{f_{s1}}{\lambda_1} - \varsigma_1 \tag{22}$$

It's time derivative is then:

$$\dot{V_1} = e_1\left(\dot{x}_{1d} - (y_2 - f_{s1})\right) + \tilde{d}_1\left(-\dot{\varsigma}_1\right) \tag{23}$$

The stabilization of e_1 can be obtained by introducing a new virtual control y_2

$$\left(y_2\right)_d = \alpha_1 = \dot{\phi}_d + k_1 e_1 + \lambda_1 \varsigma_1 \tag{24}$$

In order to compensate the effect of the velocity sensor fault of roll motion, an integral term is introduced which can eliminate the tracking error. We take:

$$\varsigma_1 = \int e_1 dt \tag{25}$$

It results that:

$$\dot{V_1} = e_1\left(-k_1 e_1 + \lambda_1 \tilde{d}_1\right) + \tilde{d}_1\left(-e_1\right) = -\begin{pmatrix} e_1 & \tilde{d}_1 \end{pmatrix}\begin{pmatrix} k_1 & -\lambda_1 \\ 1 & 0 \end{pmatrix}\begin{pmatrix} e_1 \\ \tilde{d}_1 \end{pmatrix} = -\tilde{e}_1^T Q_1 \tilde{e}_1 \tag{26}$$

k_1 and λ_1 are chosen so as to make the definite matrix positive Q_1, which means that, $\dot{V_1} \le 0$

Let us proceed to a variable change by making:

$$e_2 = \dot{x}_{1d} + k_1 e_1 + \lambda_1 \varsigma_1 - y_2 \tag{27}$$

For the second step we consider the augmented Lyapunov function:

$$V_2 = V_1 + \frac{1}{2}e_2^2 \tag{28}$$

$$\dot{V_2} = e_1\left(-k_1 e_1 + \lambda_1 \tilde{d} + e_2\right) + \tilde{d}\left(-e_1\right) + e_2\left(\beta_{s1} - b_1 u_2\right) \tag{29}$$

Such as

$$\beta_{s1} = \left(\ddot{x}_{1d} + k_1(-k_1 e_1 + e_2) + \lambda_1 e_1 - a_1 y_4 y_6 - a_2 y_2^2 - a_3 \bar{\Omega}_r y_4\right) + \Delta\beta_{s1} \tag{30}$$

and if:

$$\left|\Delta\beta_{s1}\right| = \left|k_1\lambda_1\tilde{d} + a_1(f_{s3}y_4 + f_{s2}y_6 - f_{s2}f_{s3}) + a_2(f_{s1}y_2 - f_{s1}^2) + a_3\bar{\Omega}_r f_{s2}\right| \le \lambda_2 \tag{31}$$

with: $(\Delta\beta_{s1})$ is the unknown part related to velocity sensor faults.

The control input u_2 is then extracted satisfying $\dot{V_2} \le 0$

$$u_2 = \frac{1}{b_1}\left(\ddot{\phi}_d + k_1(-k_1 e_1 + e_2) + (1+\lambda_1)e_1 + k_2 e_2 - a_4 y_2 y_6 - a_5 y_4^2 - a_6\bar{\Omega}_r y_2 + \lambda_2 sign(e_2)\right) \tag{32}$$

The term $k_2 e_2$ with $k_2 > 0$ is added to stabilize (e_1, e_2).

The same steps are followed to extract u_3, u_4, u_x, u_y and u_1.

$$\begin{cases} u_3 = \dfrac{1}{b_2}\left(\ddot{\theta}_d + k_3(-k_3 e_3 + e_4) + (1+\lambda_3)e_3 + k_4 e_4 - a_4 y_2 y_6 - a_5 y_4^2 - a_6\bar{\Omega}_r y_2 + \lambda_4 sign(e_4)\right) \\ u_4 = \dfrac{1}{b_3}\left(\ddot{\psi}_d + k_5(-k_5 e_5 + e_6) + (1+\lambda_5)e_5 + k_6 e_6 - a_7 y_2 y_4 - a_8 y_6^2 + \lambda_6 sign(e_6)\right) \\ u_x = \dfrac{m}{u_1}\left(\ddot{x}_d + k_7(-k_7 e_7 + e_8) + (1+\lambda_7)e_7 + k_8 e_8 - a_9 y_8 + \lambda_8 sign(e_8)\right) \quad /u_1 \ne 0 \\ u_y = \dfrac{m}{u_1}\left(\ddot{y}_d + k_9(-k_9 e_9 + e_{10}) + (1+\lambda_9)e_9 + k_{10} e_{10} - a_{10} y_{10} + \lambda_{10} sign(e_{10})\right) \quad /u_1 \ne 0 \\ u_1 = \dfrac{m}{\cos(x_1)\cos(x_3)}\left(\ddot{z}_d + k_{11}(-k_{11} e_{11} + e_{12}) + (1+\lambda_{11})e_{11} + k_{12} e_{12} - a_{11} y_{12} + g + \lambda_{12} sign(e_{12})\right) \end{cases} \tag{33}$$

with

$$e_i = \begin{cases} x_{id} - x_i & i \in [3,5,7,9,11] \\ \dot{x}_{(i-1)d} + k_{(i-1)} e_{(i-1)} + \lambda_{(i-1)} \varsigma_{(i-1)} - y_i & i \in [4,6,8,10,12] \end{cases} \quad (34)$$

and

$$\varsigma_i = \begin{cases} \int e_i dt & i \in [3,5,7,9,11] \\ sign(e_i) & i \in [4,6,8,10,12] \end{cases} \quad (35)$$

The corresponding lyapunov functions are given by:

$$V_i = \begin{cases} \frac{1}{2} e_i^2 + \frac{1}{2} \tilde{d}_j^2 & i \in [3,5,7,9,11] \text{ and } j \in [2,...,6] \\ V_{i-1} + \frac{1}{2} e_i^2 & i \in [4,6,8,10,12] \end{cases} \quad (36)$$

such as

$$\begin{cases} \tilde{d}_j = d_j - \varsigma_i = \frac{f_{sj}}{\lambda_i} - \varsigma_i & i \in [3,5,7,9,11] \text{ and } j \in [2,...,6] \\ Q_j = \begin{bmatrix} k_i & -\lambda_i \\ 1 & 0 \end{bmatrix} > 0 & i \in [3,5,7,9,11] \text{ and } j \in [2,...,6] \\ k_i > 0 & i \in [4,6,8,10,12] \end{cases} \quad (37)$$

To synthesize a stabilizing control laws in the presence of velocity Sensor faults, the following necessary condition must be verified:

$$|\Delta\beta_{sj}| = |\beta_{sj} - \beta_{sjn}| \le \lambda_i, \quad i \in [4,6,8,10,12] \text{ and } j \in [2,...,6] \quad (38)$$

($\Delta\beta_{sj}$) represent the unknowns parts related to velocity sensor faults.

IV. SIMULATION RESULTS

In order to evaluate the performance of the controller developed in this paper, we performed two tests simulations. In the first test, a four sensor faults f_{sj}, j∈[1,2,3,6] are added in angular velocities and linear velocity of attitude Z of our system, with 100% of these maximum values (i.e. of max($|x_i|$), i∈[2,4,6,12]) at instants 15s, 20s, 25s and 30s respectively. In the second test, the same sensor faults are added at the same previous instants, but their amplitudes are increased to 200%.
The data of this tested quadrotor are reported in appendix [9].

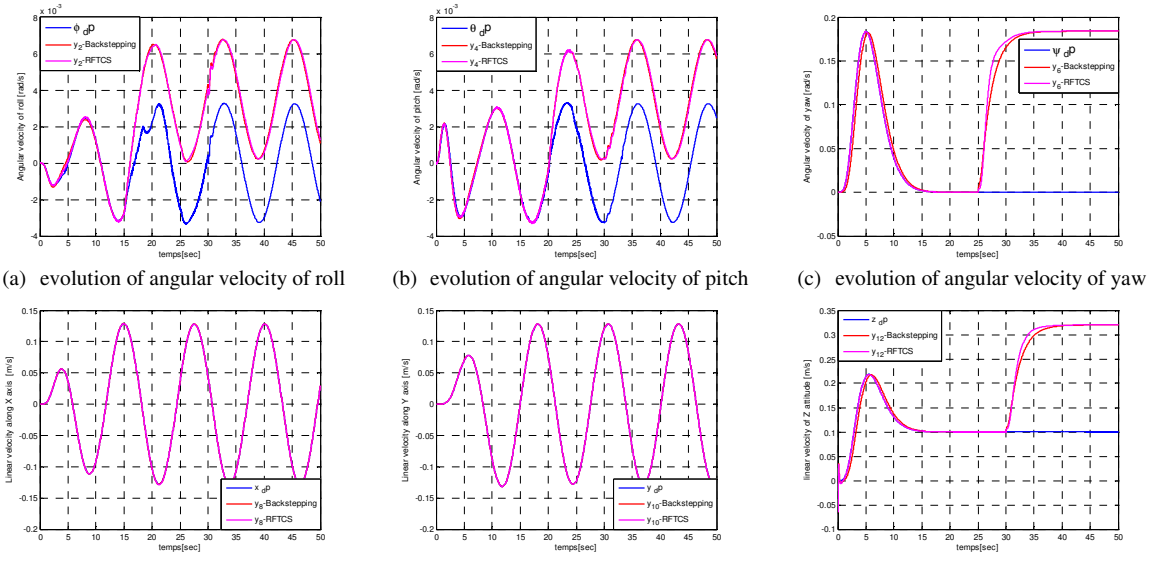

(a) evolution of angular velocity of roll (b) evolution of angular velocity of pitch (c) evolution of angular velocity of yaw

(d) evolution of linear velocity along *X* axis (e) evolution of linear velocity along *Y* axis (f) evolution of linear velocity along *Z* axis

Figure. 3. Tracking simulation results of the angular and linear velocities, Test 1.

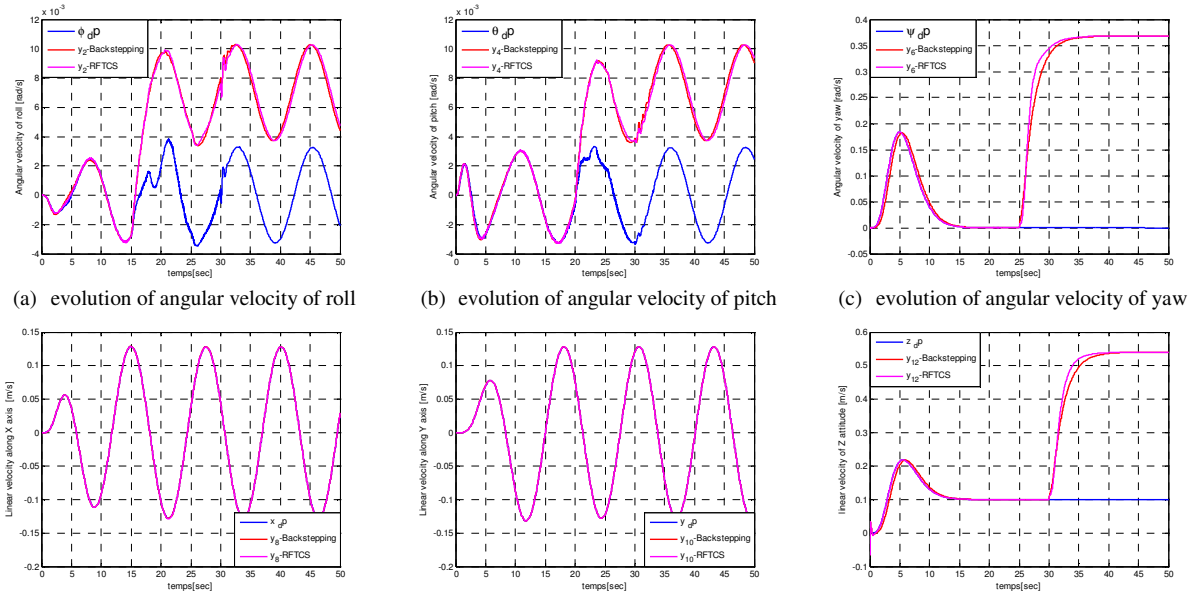

(a) evolution of angular velocity of roll (b) evolution of angular velocity of pitch (c) evolution of angular velocity of yaw

(d) evolution of linear velocity along *X* axis (e) evolution of linear velocity along *Y* axis (f) evolution of linear velocity along *Z* axis

Figure. 4. Tracking simulation results of the angular and linear velocities, Test 2.

Figure. 3 and Figure. 4 shows at outset a very good tracking of the desired velocities, but upon the appearance of sensor faults, the measurements of angular velocities and linear velocity of attitude Z (illustrated respectively by (a), (b), (c), and (f)) are deviated to their desired velocities, with 100% of her maximum values in Test. 1, and 200% of these maximum values in Test. 2 for both control strategies developed in this paper, which gives us a wrong information of the velocities of our system.

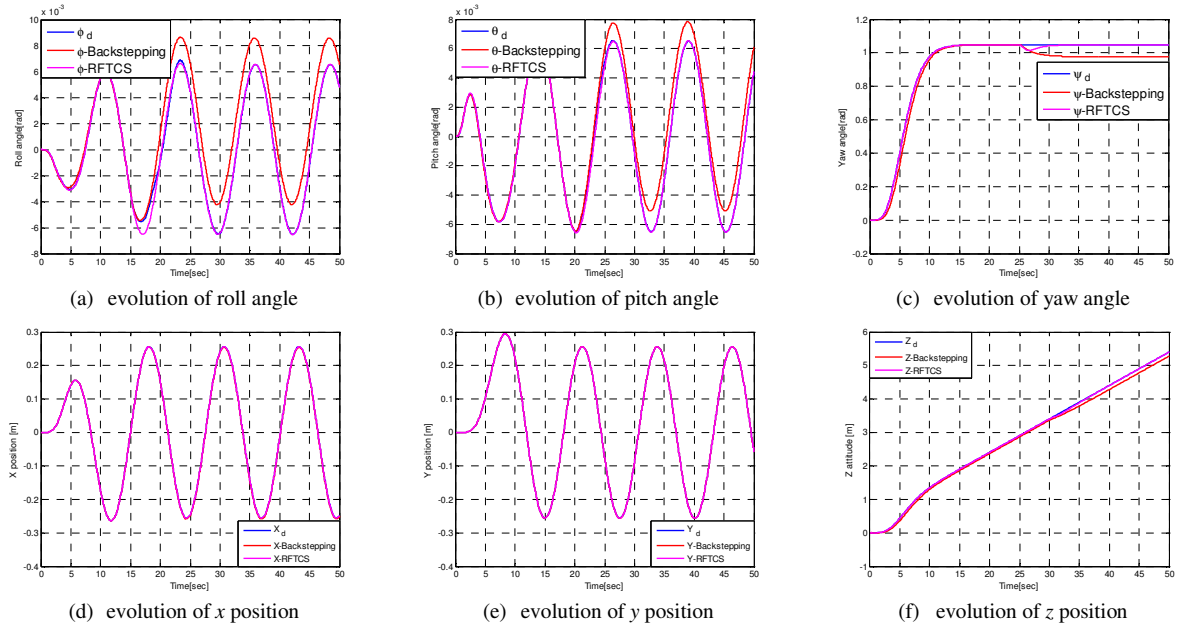

(a) evolution of roll angle (b) evolution of pitch angle (c) evolution of yaw angle

(d) evolution of *x* position (e) evolution of *y* position (f) evolution of *z* position

Figure. 5. Tracking simulation results of trajectories along roll (ϕ), pitch (θ), yaw angle (ψ) and (X,Y,Z) axis, Test 1.

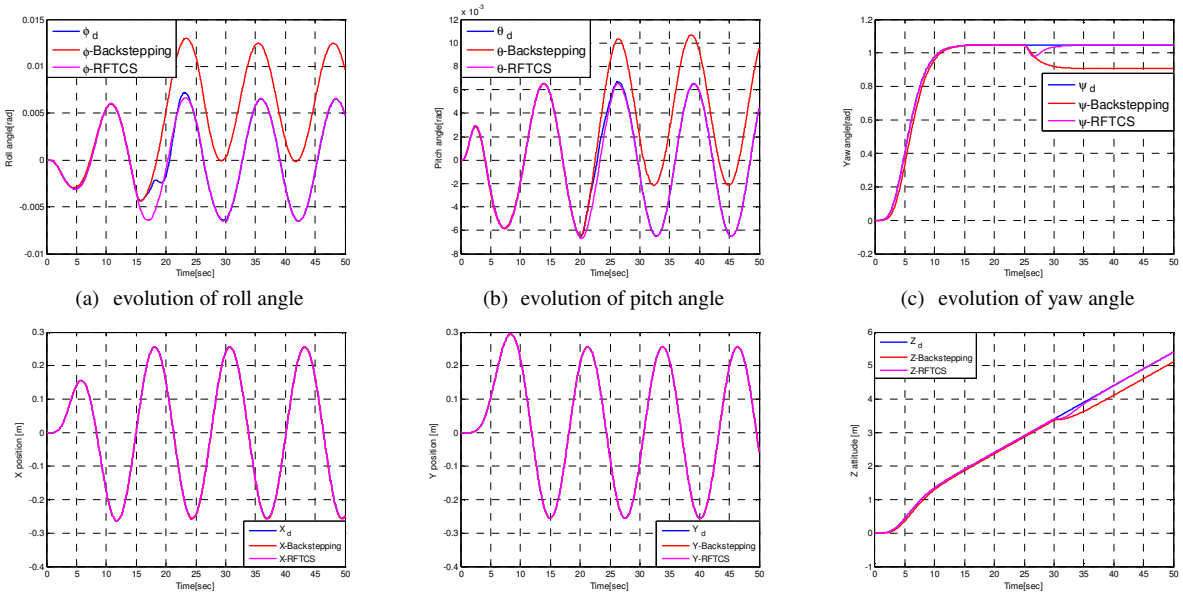

(a) evolution of roll angle (b) evolution of pitch angle (c) evolution of yaw angle

(d) evolution of *x* position (e) evolution of *y* position (f) evolution of *z* position

Figure. 6. Tracking simulation results of trajectories along roll (ϕ), pitch (θ), yaw angle (ψ) and (X,Y,Z) axis, Test 2.

According to Figure. 5 and Figure. 6, there is a very good tracking of the desired trajectories for both control strategies at outset, but after the occurrence of sensor faults in angular velocities and linear velocity of the attitude Z, the actual trajectories along roll angle, pitch angle, yaw angle, and *z* position (illustrated respectively by (a), (b), (c), and (f)) corresponding of classical backstepping approach are deviated to their desired values, which also explains the inefficiency of this control approach after occurrence of velocity sensor faults. However, the actual trajectories corresponding of this new control strategy converge to their desired trajectories after transient peaks with low amplitudes caused by the appearance of velocity sensor faults.

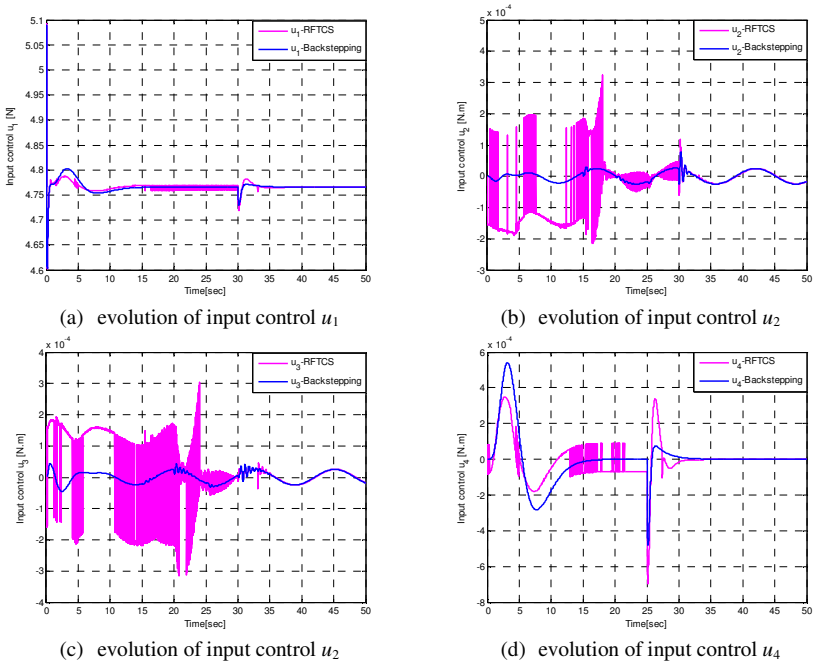

(a) evolution of input control u_1 (b) evolution of input control u_2

(c) evolution of input control u_2 (d) evolution of input control u_4

Figure. 7. Simulation results of all controllers, Test 1.

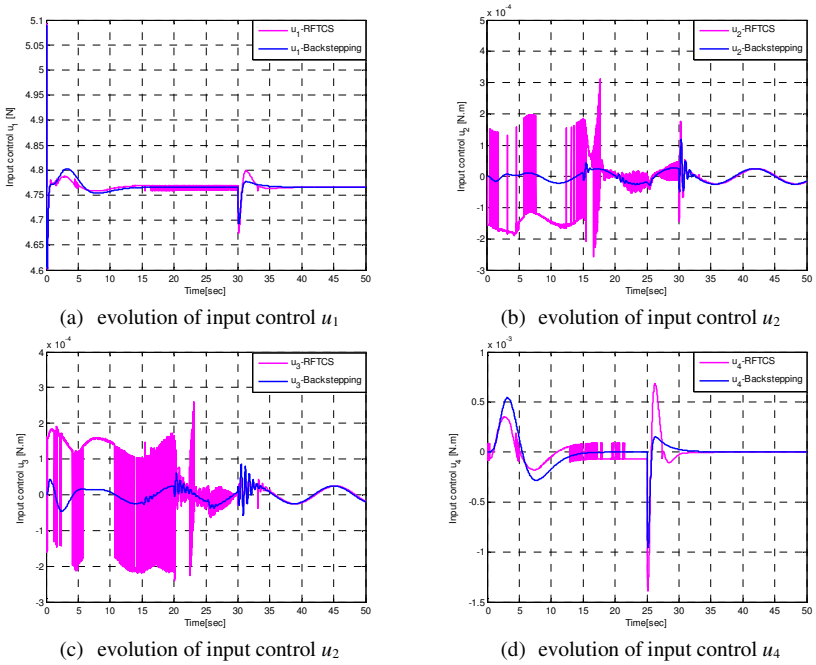

(a) evolution of input control u_1 (b) evolution of input control u_2

(c) evolution of input control u_2 (d) evolution of input control u_4

Figure. 8. Simulation results of all inputs control, Test 2.

From Figures. 7 and 8, it is clear to see that the classical backstepping approach give a smooth inputs control, with transient peaks during the appearance of sensor faults in angular velocities and linear velocity of the attitude Z, However, the inputs control corresponding to this new control strategy are characterized at outset by very fast switching caused by using of the discontinuous compensation term "sign", also with transient peaks during the appearance of velocity sensor faults, but this chattering gone after the appearance of sensor fault in linear velocity of the attitude Z.

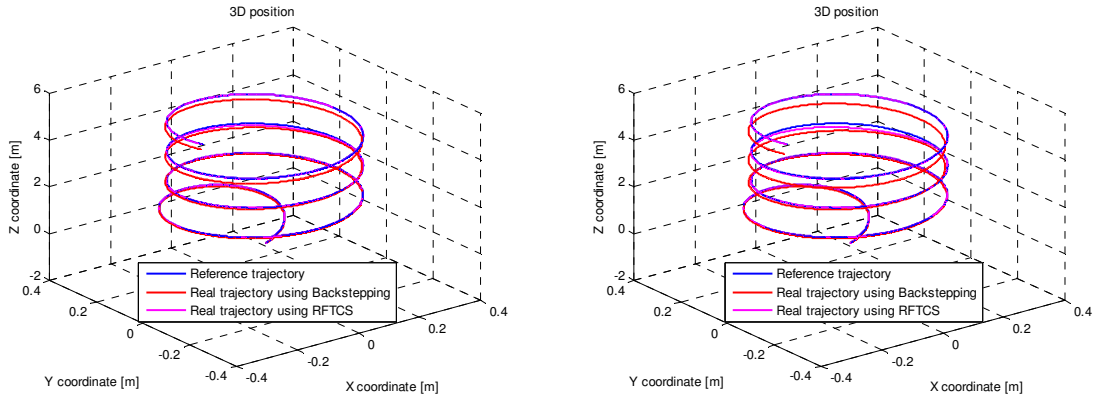

(a) evolution of position along (X,Y,Z) axis, Test 1 (b) evolution of position along (X,Y,Z) axis, Test 2

Figure. 9. Global trajectory of the quadrotor in 3D.

The simulation results given by Figure. 9 show the efficiency of the robust fault tolerant control strategy developed in this paper, which clearly shows a good performances and robustness towards stability and tracking of this control strategy with respect to the backstepping approach after the occurrence of velocity sensor faults.

V. CONCLUSION AND FUTURE WORKS

In this paper, we proposed a new strategy of fault tolerant control based on backstepping approach and including the velocity sensor faults. Firstly, we start by the development of the dynamic model of the quadrotor taking into account the different physics phenomena which can influence the evolution

of our system in the space, and secondly by the synthesis a stabilizing control laws in the presence of velocity sensor faults. The simulation results have shown that the backstepping approach renders the system unable to follow his reference after the appearance of velocity sensor faults, which also explains the sensitivity of this control technology towards a sensor failures. However, these simulation results also shows a high efficiency of the robust fault tolerant control strategy developed in this paper, she preserves performance and stability of quadrotor during a malfunction of these velocity sensors. As prospects we hope to develop other fault tolerant control strategies in order to eliminate the chattering phenomenon in the inputs control, while maintaining the performance and stability of this system with implementation them on a real system.

APPENDIX

m	0,486 kg
g	9,806 m/s^2
l	0,25 m
b	$2{,}9842 \times 10^{-5}$ $N/rad/s$
d	$3{,}2320 \times 10^{-7}$ $N.m/rad/s$
J_r	$2{,}8385 \times 10^{-5}$ $kg.m^2$
$I_{(x,y,z)}$	diag (3,8278; 3,8288; 7,6566) $\times 10^{-3}$ $kg.m^2$
$K_{fa(x,y,z)}$	diag (5,5670; 5,5670; 6,3540) $\times 10^{-4}$ $N/rad/s$
$K_{ft(x,y,z)}$	diag (5,5670; 5,5670; 6,3540) $\times 10^{-4}$ $N/m/s$
μ_0	0,0122
μ_1	6,0612
μ_2	189,63
η	280,19

REFERENCES

[1] S. Bouabdellah, P.Murrieri, & R.Siegwart. (2004) "Design and control of an indoor micro quadrotor", *Proceeding of the IEEE, ICRA*, New Orleans, USA.

[2] S. Bouabdellah, & R.Siegwart. (2005) "Backstepping and sliding mode techniques applied to an indoor micro quadrotor", *Proceeding of the IEEE, ICRA*, Barcelona, Spain.

[3] H. Bouadi, M. Bouchoucha, & M. Tadjine. (2007) "Modelling and Stabilizing Control Laws Design Based on Backstepping for an UAV Type-Quadrotor", *Proceeding of 6 the IFAC Symposium on IAV*, Toulouse, France.

[4] H. Bouadi, M. Bouchoucha, & M. Tadjine. (2007) "Sliding Mode Control Based on Backstepping Approach for an UAV Type-Quadrotor", *International Journal of Applied Mathematics and Computer Sciences*, Vol.4, No.1, pp. 12-17.

[5] M. Bouchoucha, M. Tadjine, A. Tayebi, & P. Müllhaupt. (2008) "Step by Step Robust Nonlinear PI for Attitude Stabilization of a Four-Rotor Mini-Aircraft", *16th Mediterranean Conference on Control and Automation Congress Centre*, Ajaccio, France, pp. 1276-1283.

[6] P. Castillo, A. Dzul, & R. Lozano. (2004) "Real-Time Stabilization and Tracking of a Four-Rotor Mini Rotorcraft", *IEEE Transactions on Control Systems Technology*, Vol. 12, No. 4, pp. 510-516.

[7] J. Colorado, A. Barrientos, , A. Martinez, B. Lafaverges, & J. Valente. (2010) "Mini-quadrotor attitude control based on Hybrid Backstepping & Frenet-Serret Theory", *Proceeding of the IEEE, ICRA*, Anchorage, Alaska, USA.

[8] A. Das, F. Lewis, & K. Subbarao (2009) "Backstepping Approach for Controlling a Quadrotor Using Lagrange Form Dynamics." *Journal of Intelligent and Robotic Systems*, Vol. 56, No. 1-2, pp. 127- 151.

[9] L. Derafa, T. Madani, & A. Benallegue. (2006) "Dynamic modelling and experimental identification of four rotor helicopter parameters", *IEEE-ICIT* , Mumbai, India, pp. 1834-1839.

[10] N. Guenard, T. Hamel, & R. Mahony. (2008) "A Practical Visual Servo Control for an Unmanned Aerial Vehicle", *IEEE Transactions on Robotics*, Vol. 24, No. 2, pp. 331-340.

[11] T. Hamel, R. Mahony, R. Lozano, & J. Ostrowski. (2002) "Dynamic modelling and configuration stabilization for an X4-flyer", *IFAC world congress*, Spain.

[12] W.Khalil, Dombre. (2002) "modelling, identification and control of robots", *HPS edition*.

[13] R. Lozano, P. Castillo, & A. Dzul. (2004) "Global stabilization of the PVTOL: real time application to a mini aircraft", *International Journal of Control*, Vol 77, No 8, pp. 735-740.

[14] A. Mokhtari, & A. Benallegue. (2004) "Dynamic Feedback Controller of Euler Augles and Wind Parameters Estimation for a Quadrotor Unmanned Aerial Vehicle", *Proceeding of the IEEE, ICRA*, New Orleans, LA, USA, pp. 2359-2366.

[15] J.J.E. Slotine, & W. Li. (1991) "Applied nonlinear control", Prentice Hall, Englewood Cliffs, NJ.

[16] A. Tayebi, & S. Mcgilvray. (2004) "Attitude stabilisation of a four rotor aerial robot", *IEEE Conference on Decision and Control*, Atlantis Paradise Island, Bahamas, pp. 1216-1217.

[17] A. Tayebi, & S. McGilvray (2006) "Attitude stabilization of a VTOL Quadrotor Aircaft", *IEEE Transactions on Control Systems Technology*, Vol. 14, No. 3, pp. 562-571.

Authors

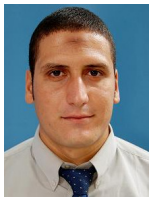

Hicham KHEBBACHE is Graduate student (Magister) of Automatic Control at the Electrical Engineering Department of Setif University, ALGERIA. He received the Engineer degree in Automatic Control from Jijel University, ALGERIA in 2009. Now he is with Automatic Laboratory of Setif (LAS). His research interests include Aerial robotics, Linear and Nonlinear control, Robust control, Fault tolerant control (FTC), Diagnosis, Fault detection and isolation (FDI).

Belkacem SAIT is Associate Professor at Setif University and member at Automatic Laboratory of Setif (LAS), ALGERIA. He received the Engineer degree in Electrical Engineering from National Polytechnic school of Algiers (ENP) in 1987, Magister degree in Instrumentation and Control from HCR of Algiers in 1992, and Ph.D. in Automatic Product from Setif University in 2007. His research interested include discrete event systems, hybrid systems, Petri nets, Fault tolerant control (FTC), Diagnosis, Fault detection and isolation (FDI).

Fouad YACEF is currently a Ph.D. student at the Automatic Control Department of Jijel University, ALGERIA. He received the Engineer degree in Automatic Control from Jijel University, ALGERIA in 2009, and Magister degree in Control and Command from Military Polytechnic School (EMP), Algiers, in November 2011. His research interests include Aerial robotics, Linear and Nonlinear control, LMI optimisation, Analysis and design of intelligent control systems.